Shockley-Queisser Triangle: An Analytical Tool for Predicting the Thermodynamic Efficiency Limits of Multi-junction Tandem and Bifacial Solar Cells

Muhammad A. Alam[a,1] **and M. Ryyan Khan**[b]

[a]School of Electrical and Computer Engineering, Purdue University, West Lafayette, IN 47906 USA ; [b]Department of Electrical and Electronics Engineering, East West University, Dhaka, Bangladesh

This manuscript was compiled on April 22, 2019

As monofacial, single junction solar cells approach their fundamental limits, there has been significant interest in tandem solar cells in the presence of concentrated sunlight or tandem bifacial solar cells with back-reflected albedo. The bandgap sequence and thermodynamic efficiency limits of these complex cell configurations generally require sophisticated numerical calculation. The analysis of specialized cases are scattered throughout the literature. In this paper, we show that a powerful graphical approach called the normalized "Shockley-Queisser Triangle", (i.e. $i_{mp} = 1 - v_{mp}$), is sufficient to calculate the bandgap sequence and efficiency limits of arbitrary complex PV topologies. The results are validated against a wide variety of specialized cases reported in the literature and are accurate within a few percent. We anticipate that wide-spread use of the SQ-triangle will illuminate the deeper physical principles and design trade-offs involved in the design of tandem solar cells under arbitrary concentration and series resistance.

| Solar cells | Thermodynamic efficiency 2 | Shockley-Queisser 3 | Scaling theory | Tandem, concentrator, bifacial cells |

The efficiency of single junction monofacial solar cells have been rising steadily over the years [3] and in some cases, they are beginning to approach the fundamental limits for single-junction solar cells predicted by Shockley-Queisser (SQ). [4] [5]. In addition, the knowledge gained from volume manufacturing has dramatically reduced the manufacturing and installation costs. Further reduction in LCOE will require continued improvement in the lifetime and efficiency of the solar cells. Therefore, it is not surprising that there has been a significant effort in improving the reliability of the modules, as well as using new cell technologies such as multijunction and bifacial solar cells [7] [9]. The intrinsic bifaciality in silicon heterojunction cell, the availability of large bandgap perovskite and organic solar cells, and lower-bandgap quantum-dot cells have encouraged experimentation involving these new cell structures and module and farm topology.

As is well known, the original SQ paper [4] offered a powerful incentive for efficiency improvement of single junction solar cells by highlighting the opportunity of efficiency gain towards its thermodynamic limit. Similar work by C. Henry [6] and others have helped define the thermodynamic limits for multijunction tandem cells. Recent work on thermodynamic limits of 2-junction (2-J) tandem cell (silicon, perovskite) [7], N-Junction bifacial solar cells, 3-J, 4-J and 5-J concentrator PV including the effect of series resistance have been discussed. Other topics involving optimization for food, water, and energy (FEW) and the hydrolysis of water by multi-junction tandem PV have also been analyzed. A literature review shows that relative performance gain of new PV concepts are nontrivial and require complicated numerical analysis. Such an analysis cannot transparently establish the functional relationship between the design parameters and ultimate photo-conversion efficiency.

In this paper, we will develop a intuitive but powerful graphical approach called Shockley-Queisser Triangle (S-Q Triangle). The approach will unify through simple scaling relationships the thermodynamic efficiency results of various types of solar cells scattered in the literature. It will also predict the efficiency limits of emerging solar cell concepts (e.g. bifical tandem solar cells) for which the thermodynamic results are unknown. More importantly, it will explain the intrinsic trends of nonlinear efficiency gain with cell number, how a two-junction bifacial tandem cell outperforms a four junction monofacial tandem cell, the effect of series resistance on the choice of cell configuration, and so on.

1. The Shockley-Queisser Triangle

The scaling analysis presented in this paper relies on two key observations related to the voltage and the current needed to produce the maximum output power of a solar cell, i.e., maximum power-point voltage (V_{mp}) and maximum power-point current (I_{mp}). At the radiative limit, V_{mp} of a solar cell with bandgap E_g is given by the exact relationship involving

Significance Statement

A solar cell converts sunlight directly to electricity and is an important source of renewable energy. The thermodynamic efficiency of a solar cell defines the ultimate limit of photo-conversion and suggests strategies to achieve it. Since modern fixed-tilt single junction solar cells coverts less than 1 in 10 photons into useful energy, a variety of alternate strategies (e.g. tandem, concentrator, bifacial cells) have been proposed. In simple, single-line scaling formula, this paper unifies isolated and scattered results derived over last 50 years and generalizes them to new technologies whose thermodynamic limits are unknown. The work will identify promising new concepts and their performance gain over traditional technologies.

[1]E-mail: alampurdue.edu

the Carnot factor η_C and the angle entropy factor Δ:

$$V_{mp} = \left(1 - \frac{T_D}{T_S}\right) E_g - \frac{k_B T_D}{q} \ln\left(\frac{1}{c}\frac{\Omega_D}{\Omega_S}\right) \qquad [1]$$

Here, T_D and T_S are the temperatures of the solar cell and the sun, respectively. The Carnot factor$\eta_C \equiv (1 - T_D/T_S) = 1 - 300/6000 = 0.95$ and the angle entropy factor, $\Delta \equiv (k_B T_D/q)\ln(\Omega_D/c\Omega_S)$, depends on the size of the solar disk (Ω_S) as viewed from earth and the angular radiation from the solar cell, i.e. $\Omega_D = 2\pi$ or 4π depending on the back reflector. Thus, $\Delta \simeq 0.31$ at one-sun concentration (i.e., $c = 1$).

Similarly, the maximum power-point current under AM1.5G illumination (I_{mp}) is given by [9]

$$I_{mp} \simeq c I_{sun}(1 - \beta' E_g) \qquad [2]$$

The current is proportional to the solar concentration, c, and I_{sun} is the projected current at $E_g \to 0$, and $\beta' \sim 4.7 k_B T_S$ is the loss-coefficient of photo-current with increasing bandgap. The linear approximation holds for $0.5\text{eV} < E_g < 2\text{eV}$. The nonlinearity of I_{mp} under arbitrary blackbody illumination is easily analyzed by a simple one-to-one mapping between E_g and its linear approximation [9].

Inserting (1) into (2), and defining $i_{mp} = I_{mp}/I_0$ and $v_{mp} = V_{mp}/V_0$, we obtain the equation for the SQ triangle, namely,

$$i_{mp} = 1 - v_{mp} eq:3 \qquad [3]$$

Here, $I_0 \equiv c I_{sun}(1 - \beta\Delta)$ and $V_0 \equiv (1 - \beta\Delta)/\beta$, with $\beta = \beta'/\eta_C$.

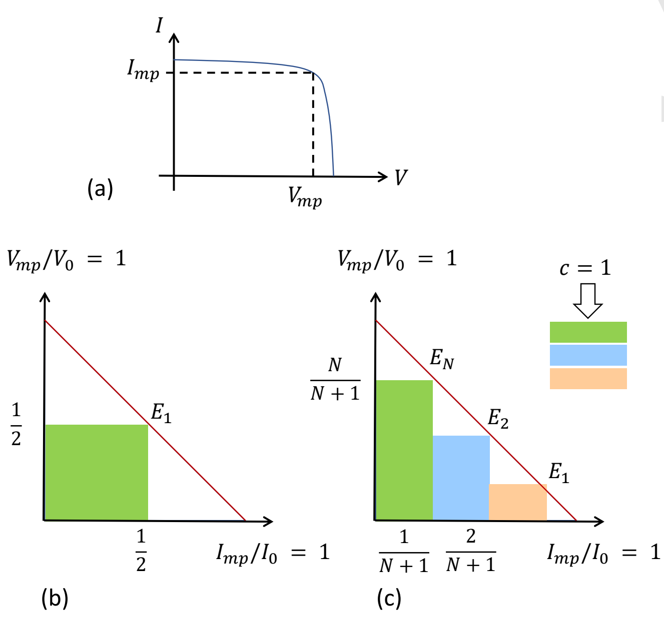

Fig. 1. (a) The I-V characteristic of a solar cell with a known bandgap E_g. The maximum power-point $(V_{mp}(E_g), I_{mp}(E_g))$ is identified. (b,c) Each point on the SQ-line represents a unique material with bandgap E_g. The axes correspond to the normalized v_{mp} and i_{mp}. The S-Q triangles for (b) single-junction ($N = 1$) and (c) triple-junction ($N = 3$) solar cells.

In Fig. 1, Eq. **??** defines the S-Q triangle. Each point on the diagonal represents a material with bandgap E_g . The analytical power of the triangle is obvious: the optimum bandgaps and the thermodynamic efficiency of an N-junction solar cell are obtained by tiling the triangle by rectangular boxes that maximize the triangle coverage. It follows that

$$V_{mp}^{\{i\}} = \frac{iV_0}{N+1}, \qquad [4a]$$

$$I_{mp}^{\{i\}} = \frac{I_0}{N+1}. \qquad [4b]$$

Once, V_{mp} is known, Eq. 1 identifies the material of interest with specific bandgap, $E_{g,i} = (V_{mp,i} + \Delta)/\eta_C$. Summing over the boxes within the SQ triangle, we find the efficiency of N-junction tandem cell with concentrated sunlight c is given by

$$\eta_N(c) = \frac{I_0 V_0}{P_{in}} \times \frac{N}{2(N+1)c} \qquad [5]$$

where P_{in} (kW/m^2) is the power input under AM1.5G illumination. Below, we will establish that the elegantly simple pair of equations (4) and (5) are accurate within a few percent to the most sophisticated numerical analysis published to date.

2. Model validation by results scattered in the literature

A. Efficiency of Single Junction PV with $c = 1$. The essential correctness of (4) and (5) can be established by calculating the optimum efficiency of a SJ cell under AM1.5G illumination. With $c = 1, N = 1$, and $I_{sun} = 83.75$ mA/cm^2, we find $I_0 = 71.916$ mA/cm^2 and $V_0 = 1.904$ V. Therefore, $\eta_1 = 34.2\%$ occurs at $V_{mp} = 1.92/2 = 0.96$ eV or $E_g = 1.34$ eV. The result is physically justified because $E_g \sim 2.7 k_B T$ is the average photon energy of the solar spectrum. Also, the results compares very well with the most accurate numerical results published in the literature, i.e. $\eta_1 = \mathbf{33.7}\%$ occurs at $E_g = 1.34$ eV [**3**]. The S-Q triangle also explains the flatness of the efficiency between $1.1eV < E_g < 1.6eV$. After all, the normalized output power obtained from $p = v_{mp} i_{mp} = v_{mp}(1 - v_{mp})$ is relatively insensitive to V_{mp} (or equivalently E_g) for wide variety of the bandgaps close to 1.34 eV.

B. Efficiency of Concentrated Solar Cells with $c = 300$. Since a SJ solar cell operates far below the Carnot limit (~95%) and only converts one-third (33-34%) of the incident energy into useful power output, many solar cell innovations since the 1960s have focused on improving the efficiency of a photovoltaic converter. One of these approaches involved using a parabolic mirror to concentrate sunlight onto a solar cell.

The calculation of efficiency limits of concentrator solar cells is difficult; the numerical results are available only for specific concentrations. Fortunately, the efficiency and bandgaps predicted by (4) and (5) hold for any arbitrary concentration, therefore the model can be validated by comparing with specific numerical results from the literature [**13**]. For example, for $c = 300$, $\Delta \equiv (k_B T_D/q)\ln(\Omega_D/c\Omega_S) = 0.16$. Therefore, $V_0 = 2.06$ V, and $I_0/c = 77.8$ mA/cm^{-2}. The corresponding efficiency $\eta_1(c = 300) = 40.2\%$ compares well with $\eta = 41.1$ reported in the literature. Also, the increase of V_{mp} to $2.06/2 = 1.03$ eV and the reduction of the bandgap to $E_g = 1.25$ eV to maximize efficiency are consistent with the values predicted by the thermodynamic calculator [8].

C. Thermodynamic Efficiency N-junction Tandem Cell. A second approach to improve the conversion efficiency of solar cells involves choosing a series of absorbers with different bandgaps so that they all produce equal amount of current. The absorbers are then connected optically and electrically in series to improve photoconversion efficiency. Traditional optimization involve an iterative search to find the bandgap-combination to maximum efficiency.

In contrast, Eq. 5 predicts that

$$\eta_N(c) = \eta_1(c) \times \frac{2N}{[(N+1)]} \qquad [6]$$

Fig. 2 compares the Eq. 6 with the most sophisticated numerical result available in the literature [6]. Table I in SI-document confirms that the maximum error between Eq. 6 and numerical predictions are within a few percent. Interestingly, Eq. 6 identifies the efficiency-gain scaling-factor for tandem cells (i.e. $2N/(N+1)$) that had been hidden in plain sight in all the numerical results. The scale-factor anticipates a well-known results that $\eta_{N\to\infty} = 2\eta_1$. Graphically, the triangle in Fig. 1(c) is fully tiled with boxes for $N \to \infty$. The triangle has the double the area single square in Fig. 1(b). Finally, although the scale-factor is specifically derived for AM1.5G, it captures the essential scaling trends in other spectrum (including Black-body radiation) as well, see SI.

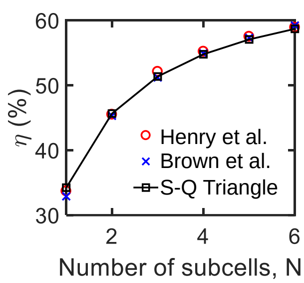

Fig. 2. The simple N-dependence predicted by (5) is validated by monofacial and bifacial tandem data taken from **Ref.** [9].

In addition, for $N = 3$ the maximum power point voltages given by Eq. 4 are: 0.48V, 0.96V, and 1.44V. The corresponding bandgaps are given by (1): 0.83 eV, 1.33 eV, and 1.84 eV. The results are within 0.1-0.2 eV of the results reported in the literature [13]. The deviation reflects the nonlinearity of I_{mp} vs. E_g curve and the slight variation in the spectrum. The power of the SQ approach is now obvious: Eq. 6 anticipates the nonlinear dependence of η_N vs. N and predicts the bandgaps for any arbitrary N-junction tandem cell.

D. Thermodynamic Efficiencies of four and five junction concentrator tandem cells with $c = 300$. The conversion efficiency is further improved in a tandem cell is placed under concentrated sunlight. Once again, the numerical optimization is so difficult that they have been reported for only a few specialized cases. The optimum bandgaps to maximize efficiency is obtained by an time-consuming iterative search over the bandgap space. Since (4) and (5) apply to any N-junction tandem cell under arbitrary illumination, we can confirm its validity by comparing to a few specific results for 4-junction and 5-junction [13] cells. Table II and Fig. 3 show that both the bandgap sequence and the thermodynamic efficiencies compare well with the values reported in the literature.

E. The Effect of Series Resistance on Concentrated Solar Cell . The early design of concentrator solar cells highlighted

Table 1. Effect of concentration on optimized bandgaps.

$N=4, c=300$							
	1	2	3	4		I_{mp}	η
V_{mp}	0.41	0.82	1.23	1.65		16.3	63.5
E_g	0.60	1.04	1.47	1.90			63.5
E_g[13]	0.52	0.97	1.38	1.89			63.7
$N=5, c=300$							
	1	2	3	4	5	I_{mp}	η
V_{mp}	0.34	0.69	1.03	1.37	1.71	12.9	66.2
E_g	0.53	0.89	1.25	1.61	1.98		66.2
E_g [13]	0.52	0.92	1.21	1.57	2.03		66.2

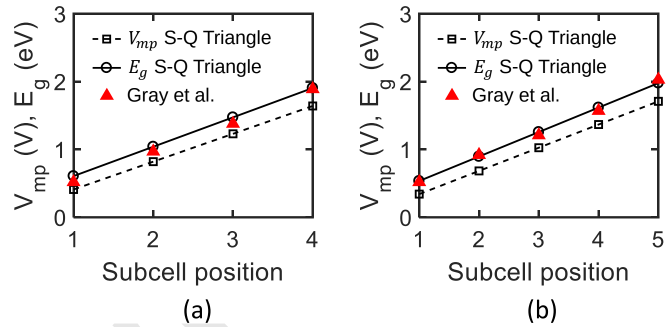

Fig. 3. The analytical results predicted by Eqs. 4-6 compared to the numerical results published in the literature. (a) Four junction tandem cell. (b) Five junction tandem cell.

the need to account for the voltage drop in the series resistance with in response to extremely large current in these systems. Once again, the problem is solved iteratively and maximum efficiency associated with a specific series resistance is not known.

The discussion in previous sections suggests that $\eta(c)$ increases monotonically with c, the solar concentration, see (5). In practice, the series resistance, R_s, reduces the efficiency beyond a critical concentration, c_{crit}. Here, Eq. 1 can be rewritten as $V_{mp} = V_{mp}(R_s = 0) - \alpha I_{mp} R_s$ to account for R_s. Once again, the S-Q triangle is constructed by inserting the expression for V_{mp} into (2), so that (3) can now be rewritten with the following parameters: $I_0 \equiv cI_{sun}(1-\beta\Delta)/(1+cI_{sun}\beta\alpha R_s)$ and $V_0 \equiv (1-\beta\Delta)/\beta$. The triangle is renormalized, but all the equations remain the unchanged.

With the renomalized axes, Eq. 5 anticipates the efficiency of a concentrator solar cell as a function of R_s and c, shown as a contour plot in Fig. 4(a). The concentration-dependent efficiencies have been reported for $R_s = 0.01\ \Omega\ \text{cm}^-2$ and $R_s = 0.05\ \Omega\ \text{cm}^-2$. These values correspond to the two horizontal lines in Fig. 4(a). Fig. 4(b) shows that the analytical results from Eq. 5 (open symbol) match very well the numerical results (filled symbols) reported in the literature.

Interestingly, Fig. 4(a) and 4(b) anticipate a reduction in η beyond c_{crit}. By maximizing Eq. 5, we find

$$\frac{C_{crit}^{-1}}{I_{sun} R_s \alpha} = \beta\left[\frac{(1-\beta\Delta)^2}{2\beta v_T} - 1\right] \sim \frac{0.85}{2v_T} \qquad [7]$$

For $N = 3$, $\alpha = 1.4\times10^{-4}$ is a fitting parameter. For, $R_s = 0.01\Omega cm^{-2}$, $c_{crit} = 528.1$; for $R_s = 0.05\Omega cm^{-2}$,$C_{crit} = 110.$ 2. In other words, $C_{crit} \propto R_s^{-1}$. The corresponding efficiencies by (5) are 58.32 and 56.1%, respectively.

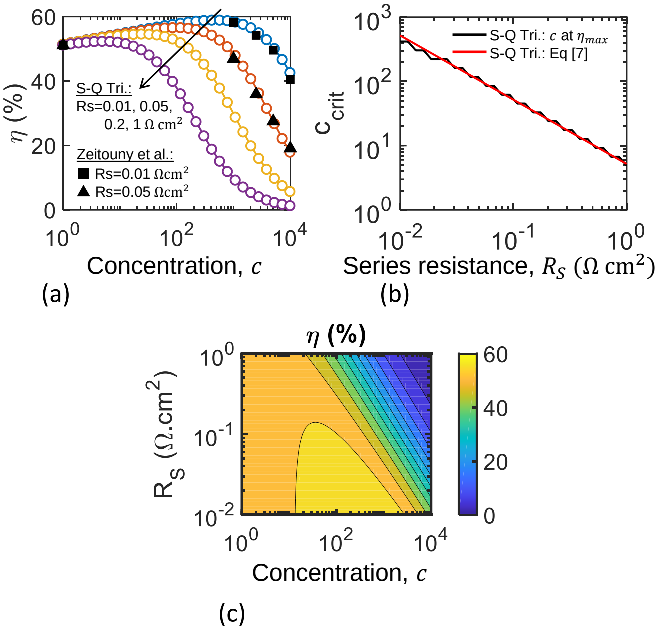

Fig. 4. The predictions from Eq. 7 is compared with the numerical results from [14] for a triple junction solar cell. (a) The efficiency contour plots as a function of series-resistance and solar concentration. (b) The turn-around of efficiency a function of solar concentration is accurately anticipated by Eq. 7.

3. Bifacial Tandem Solar cells: An Emerging Solar Cell Technology

Although the bifacial solar cell concept originated in the 1980s, recent technological innovations have made it competitive compared to monofacials. The bifacial panels are expected to capture 30% of the market share by 2030 [REF: ITRPV, 2018]. Despite its significant implications, the general thermodynamic limit of bifacial solar cell is not known [9]. In this section, we show that the S-Q triangle not only captures the scaling trends, but also explains intuitively an unexpected discontinuous jump in efficiency when the cell number exceeds a critical value, N_{crit}.

Fig. 5 shows the generalization needed to calculate the efficiency of a bifacial tandem cell. The extended triangle accommodates the cells illuminated both from the top and the bottom. An interesting aspect of bifacial cells is that depending on the albedo, the cell with the smallest bandgap E_0 may have to be placed in the middle of the stack, i.e. there are U cells above and D cell below the $E_0 - cell$, so that $N = U + D + 1$.

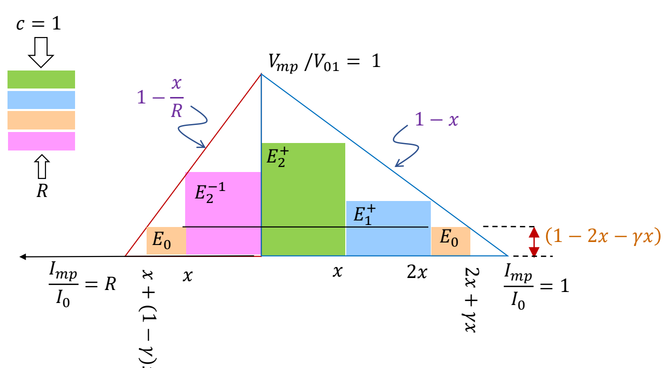

Fig. 5. The analytical results predicted by Eqs. 4-6 compared to the numerical results published in the literature. (a) Four junction tandem cell. (b) Five junction tandem cell. solar cells can be optimized with an extended SQ triangle, where the bottom cell uses the albedo light.(top) For $N < N_{crit}$; (bottom) $for N > N_{crit}$.

The sum of the boxes gives the power output:$S_N(U, D, R)$

$$s_N = \sum_{i=1}^{U} x\,(1 - ix) + \sum_{j=1}^{D} x\left(1 - \frac{jx}{R}\right) + x(1 - Ux - \gamma x)$$
$$= Nx - x^2 Aeq : 8 \qquad [8]$$

Here,

$$\gamma \equiv (1 + D - Ux)/(1 + R) \qquad [9]$$

and

$$A \equiv \frac{U(U+1)}{2} + \frac{D(D+1)}{2R} + \frac{N}{1+R} \qquad [10]$$

The power is maximized for the current

$$\frac{I_{mp}}{I_0} \equiv x_0 = \frac{N}{2A} \qquad [11]$$

$$\frac{\eta_N}{\eta_1} = \frac{s_N}{s_1} = 2N\ x_0 \qquad [12]$$

Also, $ds_N/dU = 0$, for a fixed N and R defines the number of cells in the upper stack, U:

$$U = \frac{2N - R - 1}{eq : 13[13]}$$

Equations 9-?? (9)-(13) define the maximum power from a stack of N cell illuminated by albedo R, see **Table 4** in SI document. Describe figure. . .

In addition, (8) reduces to limiting expressions: $\eta_1(U = 0, D = 0, R) = (1+R)\eta_1(R)$ and $\eta_N(U, D = 0, R = 0)/\eta_1(R = 0) = 2N/(N+1)$, see (6). The gain gradually diminishes at higher N as larger bandgap boxes tile the original triangle, consistent with Fig. 2. The triangles anticipate that the bottom cell can have the smallest bandgap (i.e. $E_2 \geq E_1$) provided $N \leq N_{crit} \equiv 1 + R^{-1}$ [9]. This sudden change in the optimum tandem topology (and the corresponding discontinuous jump in the efficiency) has no equivalence in traditional solar cells.

Inserting (8) into 7(b), we find that for $N > N_{crit}$ and $D > 0, R \neq 0$):

$$\frac{\eta_N}{\eta_1} = \frac{8R(1+R)N^2}{2R(2N^2 + 4N - 1) - R^2 - 1}, \qquad [14]$$

and for $N < N_{crit}, D = 0$, the corresponding equation is

$$\frac{\eta_N}{\eta_1} = \frac{2(1+R)N}{2 + (N-1)(1+R)}. \qquad [15]$$

The expression reduces to the limiting case of traditional tandem cell for $R = 0$. Eqs. 14 and 19 compare well with the numerical results published previously. **[9]**

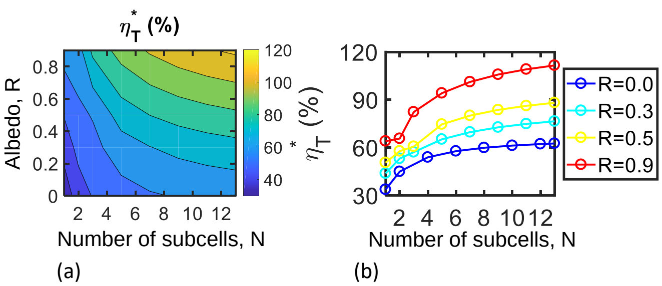

Fig. 6. (a) Efficiency gain of a bifacial-tandem solar cell depends on the number of cells in the stack (N) and the albedo parameter (R). (b) A replot of (a) to show how the efficiency increases with N and R.

4. Discussion: Thermodynamic Limits of Non-ideal Solar Cells

In Sections 2 and 3, we used the S-Q triangle method to calculate the thermodynamic (radiative) limit of ideal single-junction, tandem, bifacial, and concentrator solar cells. The results establish S-Q triangle as a powerful tool to calculate the fundamental efficiency limits of a wide variety of cell technologies.

In practice, it is sometimes helpful to modify the S-Q analysis to calculate the corresponding "practical" thermodynamic limit that accounts for material-specific losses (e.g incomplete absorption in materials with finite thickness, non-radiative losses, self-heating, etc.) In this section, we show that the S-Q triangle can predict the performance of these cells as well. Indeed, the results in the literature are special cases of our general results.

A. Imperfect EQE and ERE in a tandem solar cell . A solar cell cannot convert all the incident above-bandgap photons to useful photo-current. For a single junction device, we can write:

$$I_{mp(L)} = \eta_Q \; I_{mp} \qquad [16]$$

where η_Q is the average external quantum efficiency (EQE) which accounts for the combined effects of imperfect absorption in finite-thickness cell and the loss due to the failure of photogenerated carriers to reach the contact due to electron-hole recombination. In addition, all solar cells suffer from non-radiative recombination. This reduces the steady-state carrier concentration and photon density inside the device. The lower photon density translates to a lowered external radiative efficiency (ERE). Therefore, V_{mp} is simultaneously affected by imperfect EQE and ERE, namely [16],

$$V_{mp(L)} = V_{mp} - \frac{k_BT}{q}\ln\frac{1}{\eta_R} - \frac{k_BT}{q}\ln\frac{1}{\eta_Q} \qquad [17]$$

For high efficiency solar cells, $\eta_Q \sim 1$, therefore we need not consider for EQE explicitly in calculating the practical thermodynamic limit of a solar cell. We also know that $\eta_R < 1\%$ for indirect bandgap semiconductors or $\eta_R \sim 10-20\%$ for direct bandgap semiconductors. The following analysis accounts for the imperfect ERE.

Imperfect ERE due to non-radiative recombination reduces the operating voltage by

$$\Delta V_R = \frac{k_BT}{q}\ln\frac{1}{\eta_R} \qquad [18]$$

For example, $\Delta V_R \approx 130$ mV for Si cells , and $\Delta V_R \approx 40$ mV for high efficiency GaAs cells [**17**]. Since each material has a different ΔV_R,therefore v_{mp} of the i-th subcell of a tandem cell will be reduced by $\Delta_i = \Delta V_R/V_0$. We can now rewrite the normalized output of the bifacial tandem cell including the effect of non-radiative recombination as follows:

$$s_{N(L)} = s_N - x\sum_{i=-D}^{U}\Delta_i - x\Delta_0 \qquad [19]$$

where, s_N is the output when η_R is 100% in all subcells. Maximizing $s_{N(L)}$ with respect to x defines the optimum bifacial tandem configuration.

For example, consider a conventional tandem solar cell where Δ is the ERE-loss of the subcells. By setting $ds_{N(L)}/dx = 0$, we find:

$$\frac{I_{mp}}{I_0} = x_0 = \frac{1-\Delta}{(N+1)} \qquad [20]$$

and $\max\{s_{N(L)}\} = s_{N(L)}(x = x_0)$.

For $\eta_R = 1$, $\Delta = 0$. Inserting the limit in Eq. 19,

$$\max\{s_{N(L)}\} = \frac{N}{2(N+1)}, \qquad [21]$$

we recover the ideal limit Eq. 5, as expected.

B. Effect of temperature: cell to panel. The efficiency of the fielded solar cells reduce significantly due to self-heating, and yet the classical S-Q analysis of a solar cell presumes $T_D = 300K$ regardless the concentration of the incident light or cooling strategy. In practice, a single-junction solar cell illuminated by AM1.5G illumination and cooled by ambient convection must necessarily operate at least 15 °K over the ambient temperatures. This reflects cell self-heating associated with thermalization of above bandgap photons. Parasitic sub-bandgap absorption as well as imperfect ERE increase self-heating further. The (heat) flux balance between power absorbed and power extracted is given by

$$P_0(1-R_{PV}) = \eta_N P_0 + h(T_D - T_A) \qquad [22]$$

Here, R_{PV} is the reflection-loss, η_N is the efficiency of electrical conversion, and, h is coefficient of convective heat transfer proportional to the temperature difference between the ambient (T_A) and the device (T_D).

Self-heating reduces the efficiency of a solar cell below the (STC) as follows:

$$\eta_N(T) = \eta_N(STC) \times [1 + \beta_T(T_D - T_A)] \qquad [23]$$

where, β_T is a temperature coefficient. (e.g. $\beta_T = -0.41\%/K$ for Si PV).

C. Non-optimum E_g in tandem PV. In all the previous discussions, we have assumed that the subcell bandgaps have been chosen to maintain current matching among the cells. In practice, one may not be able to integrate optimum bandgap materials into a single stack. What would be the output power if the subcell currents are mismatched?

In general, for an N-junction conventional tandem, the current is limited by the subcell with the lowest current contribution (i.e., the one which has the lowest absorption):

$$s_N = [\sum_{i=1}^{N} v_i] \times \min\{x_i\} \qquad [24]$$

where, the normalized voltage of the i-th subcell is v_i. Once one has chosen a sequence of bandgaps the set of $\{v_i\}$ is defined. We can then find the corresponding current i_{mp} (from Eq. 5) and x_i:

$$x_i = x_{i+1} + v_{i+1} - v_i \text{and,}$$
$$x_N = 1 - v_N$$

5. Conclusions

The S-Q triangle offers an efficient and powerful technique to derive the thermodynamic efficiency limits of variety of classical (e.g. single junction, tandem, and concentrators cells) and emerging (e.g. bifacial tandem cells) technologies. The sequence of optimum bandgaps, the thermodynamic limits of currents and voltages are easily derived and can serve as an intuitive check of the experimental data. The approach provides, as a function of subcell number, a scaling justification for the improvement in the tandem cell efficiency and abrupt increase in bifacial tandem cell efficiency. Moreover, the approach is easily modified to approximately account for the non-ideal effects related to finite absorption, radiative and non-radiative recombination.

ACKNOWLEDGMENTS. We acknowledge Reza Asadpour, Tahir Patel, Profs. Mark Lundstrom, Peter Bermel, and Jeff Gray for carefully reading of and thoughtful suggestions regarding the manuscript.

1. O. Miller, E. Yablonovitch, and S. R. Kurtz. "Strong internal and external luminescence as solar cells approach the Shockley-Queisser limit."*IEEE J. of Photovoltaics*, vol. 2, p. 303, 2012.
2. X. Wang et al. "Design of GaAs solar cells operating close to the Shockley-Queisser limit."*IEEE Journal of Photovoltaics,* vol. 3, pp. 737-744, 2013.
3. M. Green, K. Emery, Y. Hishikawa, W. Warta & E. Dunlop (2015). Solar cell efficiency tables (Version 45). *Progress in photovoltaics: research and applications*,, vol. *23*, pp.1-9. 2015.
4. W. Shockley, and H. J. Queisser. "Detailed balance limit of efficiency of p-n junction solar cells."*Journal of applied physics*, vol. 32.3, pp. 510-519, 1961.
5. LC Hirst and NJ Ekins-Daukes, " Fundamental losses in solar cells",*Prog. Photovoltaics* vo. 19, p. 286, 2011.
6. C. Henry, "Limiting efficiencies of ideal single and multiple energy gap terrestrial solar cells." *Journal of applied physics* , vol. 51, pp. 4494-4500, 1980. .
7. R. Asadpour, RVK Chavali, M. R. Khan, and M. A. Alam. "Bifacial Si heterojunction-perovskite organic-inorganic tandem to produce highly efficient (? T*? 33%) solar cell."*Applied Physics Letters,* vol. 106, 243902, 2015.
8. M. R. Khan, X. Jin, and M. A. Alam. "PVLimits: PV thermodynamic limit calculator." (2016).
9. M. A. Alam, and M. R. Khan. "Thermodynamic efficiency limits of classical and bifacial tandem solar cells: An analytical approach." *Applied Physics Letters*, vol. 109, 173504, 2016.
10. E. Gençer et al., "Directing solar photons to sustainably meet food, energy, and water needs."*Sci. Rep.s* , vol. 7, 3133, 2017.
11. M. Patel, M. Khan, and M. Alam. "Thermodynamic limit of solar to fuel conversion."*arXiv preprint: 1707.03970*, (2017).
12. J. D. McCambridge, et al. "Compact spectrum splitting photovoltaic module with high efficiency."*Progress in Photovoltaics: Research and Applications* 19.3 (2011): 352-360.
13. J. Gray and J. R. Wilcox. "The design of multijunction photovoltaic systems for realistic operating conditions." In *56th IEEE Int. Midwest Symp. on Circuits and Systems,* 2013, p. 697.
14. J. Zeitouny, et al. . "Band gap engineering of multi-junction solar cells: effects of series resistances and solar concentration." *Sci. Reps* 7, p. 1766, 2017. Also see, H. Cotal, " III-V Multijunction solar cells for CPV," *Energy Environ Sci.* 2, pp. 173-192, 2009.
15. Thermodynamic Limits of Solar Cells with Non-ideal Optical Response M. Ryyan Khan, Peter Bermel, and Muhammad A. Alam
16. A. Polman and H. A. Atwater, Photonic design principles for ultrahigh-efficiency photovoltaics, Nat Mater, vol. 11, no. 3, pp. 174–177, Mar. 2012.
17. M. R. Khan, P. Bermel, and M. A. Alam, Thermodynamic limits of solar cells with non-ideal optical response, in Photovoltaic Specialists Conference (PVSC), 2013 IEEE 39th, 2013, pp. 1036–1040.